HiRISE OBSERVATIONS OF NORTH POLAR STRATIGRAPHY AND IMPLICATIONS FOR GEOLOGIC HISTORY K. E. Fishbaugh[1], K. Herkenhoff[2], S. Byrne[3], P. Russell[4], A. McEwen[3], C. Hansen[5], and the HiRISE Team. [1]International Space Science Institute (ISSI), Hallerstrasse 6, Bern CH-3012 Switzerland, fishbaugh@issibern.ch. [2]U.S. Geological Survey, Astrogeology Team, 2255 N. Gemini Dr., Flagstaff, AZ 86001, USA. [3]Lunar and Planetary Laboratory (LPL), University of Arizona, 1621 E. University Blvd., Tucson, AZ 85721, USA. [4]Physikalisches Institut, Universität Bern, Siedlerstrasse 5, CH-3012, Bern, Switzerland. [5]Jet Propulsion Laboratory, 4800 Oak grove Dr., MS 169-237, Pasadena, CA 91109, USA.

Introduction: In this study, we describe the stratigraphy of Planum Boreum, the north polar topographic dome, including: the basal unit, the classic polar layered deposits (NPLD), and the residual ice cap (NRC) at high resolution using MRO HiRISE images. From these observations, we propose a recent geologic history of the martian north polar region.

The Basal Unit: The detailed stratigraphy of the north polar basal unit is described in detail in [1]. The basal unit (also known as the Scandia Region Unit [2] and divided into several sub-units [3]) lies stratigraphically between the Hesperian-aged Vastitas Borealis materials and the Amazonian-aged NPLD and thus formed during a time when deposition of classic polar layered deposits was less favored than deposition of basal unit materials. Alternating layers of dark material and brighter, likely ice-rich material comprise this unit [4, 1]. Reworking of the dark material into dune and ripple forms [5, 1], extensions of dark material directly feeding dunes [5], and the presence of cross-bedding [1] indicate that the dark layers are sand-rich and that the basal unit is the source of the north polar sand sea [6, 7, 5], the largest erg on Mars. Mass wasting and eolian reworking dominate current erosion of the basal unit [1].

Upper and Lower Sections of the NPLD: Based on HiRISE observations of expansive, steep exposures of NPLD at the head of Chasma Boreale and along the margin of the Olympia lobe (centered at 180°W), we divide the NPLD into two sections [4]. The lower section appears similar to the polygonally fractured bright layers in the basal unit [4, 1], whereas the upper section exhibits no such polygonal fracturing (Fig. 1). The lower NPLD is typically exposed on steeper slopes, indicating a different resistance to erosion and/or more effective mass wasting by break off of blocks produced by the polygonal fracturing there. This mass wasting of the lower NPLD may be enhanced by erosion of the basal unit and by undercutting of the lower NPLD [7, 4, 1]. We cannot exclude the possibility that the fractures in the lower NPLD were formed during erosion of the scarps and thus do not extend into the bulk of the lower NPLD. Yet SHARAD data exhibit more radar layers in the upper ~600m of the NPLD than in the ~1400 m of the NPLD below that [8], indicating that these sections of the NPLD differ in dielectric properties, and hence possibly in composition and/or density. We suggest that the polygonal fracturing of the lower NPLD has resulted from a difference in material properties from the upper NPLD or from historical processes not experienced by the upper NPLD [4].

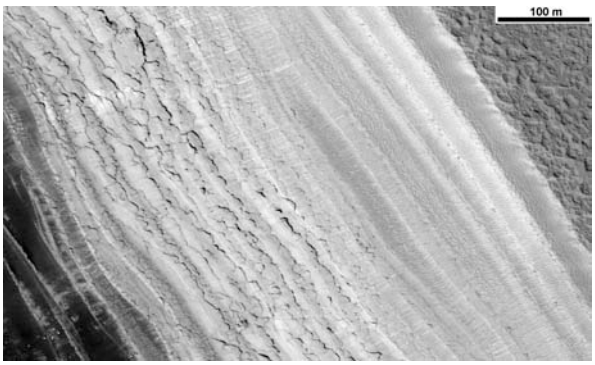

Fig. 1. Example of polygonal fracturing within the lower NPLD (left side of image) and an absence of polygonal fracturing in the upper NPLD just above (right side of image). Image PSP_001550_2640, illumination from the lower left.

NPLD Layer Thicknesses: The lower-relief troughs within the inner NPLD typically expose layers in the upper, unfractured section. It has long been assumed that orbital/axial variations and the changes in insolation and martian climate that they induce control deposition of the NPLD layers [9-11]. Thus, these layers may represent the most complete existing record of recent martian climate change, making a detailed characterization of their stratigraphy of crucial importance to Mars science. Images from the HiRISE camera are revealing unprecedented detail in these polar layers.

Layers within Viking and MGS MOC images range in apparent thickness down to the limit of image resolution, so it has been expected that the

same might be true in HiRISE images. However, we find that the apparent layer thickness range down to the limit of HiRISE resolution (30 cm/pix) only where foreshortened on relatively steep slopes [4]. Therefore, on more typical trough slopes, HiRISE has resolved the thinnest layers visible from orbit (~1 m apparent thickness, ~10 cm true thickness). Any existing, thinner layers appear to be obscured in many places by surficial deposits of frost/ice (white in Fig. 2) and dust (red in Fig. 2).

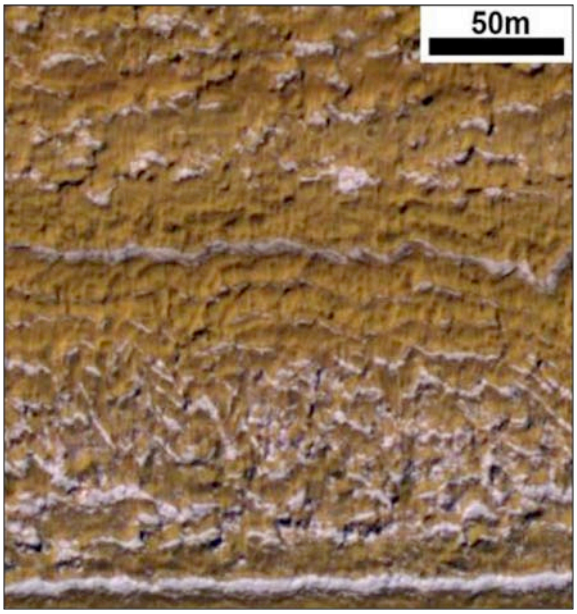

Fig. 2. Close-up example of NPLD layers (HiRISE false color, PSP_001738_2670), illustrating that each layer does not possess an obvious, inherent albedo and color but rather that frost and dust deposition is largely controlled by local and small-scale topography.

NPLD Layer Stratigraphy and the Marker Bed: We begin our preliminary analysis of upper NPLD small-scale stratigraphy with HiRISE image PSP_001488_2665 (see Fig. 3 for context), because it contains arguably the most famous layer within the NPLD: the marker bed (MB), so named because of its easily recognized, knobby texture [12]. It has been suggested that the MB represents a major lag deposit, formed during a time of net NPLD ablation [11]. However, if the NPLD have a composition of only a few percent dust, and thus ~99% ice [13-15], then 850 m of NPLD material would have to ablate in order to form the 8.5 m thick MB (taking into account MOLA-derived slope) as a dust-rich ablation lag. We find this to be unlikely.

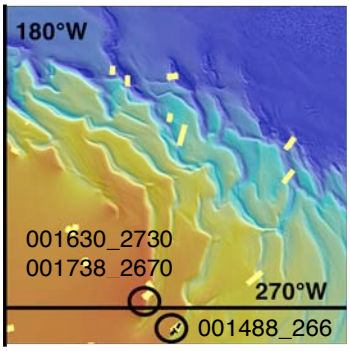

Fig. 3. Context MOLA shaded relief map showing the locations of images referred to in the text. Yellow boxes show locations of other nearby HiRISE images.

At high resolution, the MB appears as a relatively dark, massive bed with a faintly-visible drape-like texture (Fig. 4c), which could be erosional in nature, could indicate barely visible layering within the MB itself, or could be due to slumping of a surface dust lag covering. Superposed on the bed are thin, linear grooves which might be made up of chains of tiny pits. These lineations extend into the surrounding material, but they are more pronounced within the MB itself; thus, the MB is particularly susceptible to the erosion (presumably eolian) that is creating these lineations. Bounding the MB at the top are barely visible, tiny knobs and pits. The characteristic knobby texture of the MB as seen in MOC images [12, 16] is apparently caused by fingers of the layer below reaching into it.

Surprisingly, we have identified 4 layers within image PSP_001488_2665 and 6 layers within the nearby PSP_001738_2670 that closely resemble the famous marker bed in albedo, surface texture, and morphology [4]. Fig. 4 shows examples of these marker bed-like layers. Because fingers of the layers below do not extend up into the other marker bed-like layers, they do not have the distinctive knobby texture of the MB, making them previously unrecognized in lower resolution MOC images. The existence of several similar layers at various stratigraphic locations is a strong indication of a repeating climate signal; we are investigating the origin of these layers.

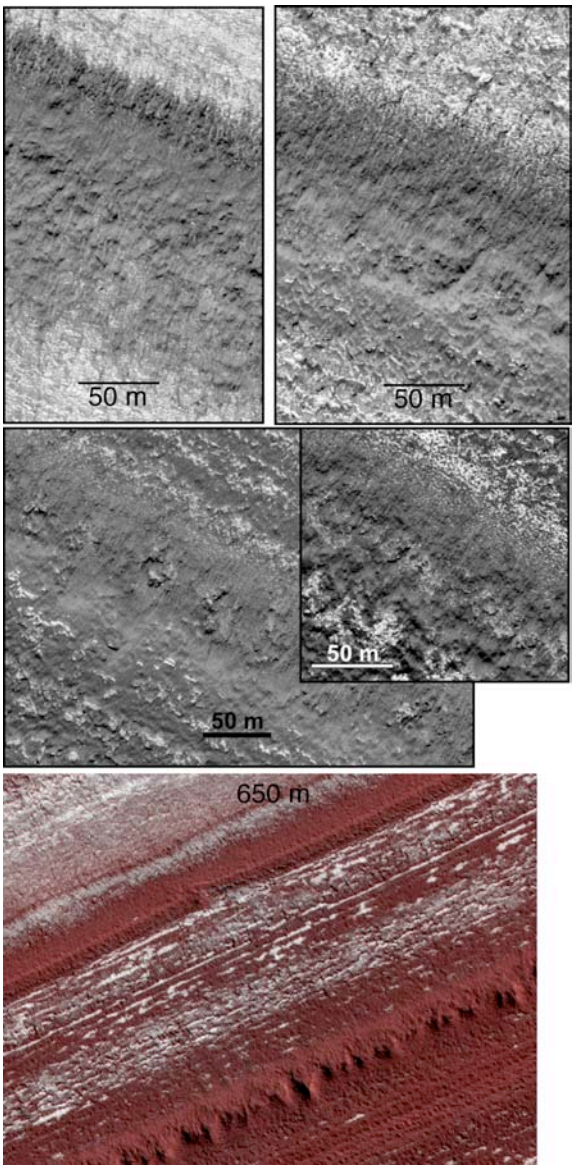

Fig. 4. Examples of the original marker bed (MB in the text) and other marker bed-like layers from image PSP_01488_2665 (A-B), from PSP_01738_2670 (C-D), and from PSP_001630_2730 (E). The original marker bed is pictured in C and E. Illumination is from the lower right.

Indications of repeating climate signals can also come in the form of repeating packages of thin layers (Fig. 5). There are two such packages in image PSP_01488_2665. Each layer is ~10 cm in thickness in the upper set and ~10-40 cm in the lower set. Keeping in mind that this is speculative, if we assume a deposition rate of 0.5 mm/yr [10], then one 10 cm layer would represent 200 years of deposition and the entire upper package 20 Kyr. These layers grow thinner and thinner towards the top of each stack. This apparent decrease in thickness could be due to the fact that the top layers are indeed thinner, that the lack of contrast there makes it difficult to distinguish layers, or that the bright material is frost which is obscuring the layers. It is possible that the two layer sets, separated by ~18 m (36 Kyr at 0.5 mm/yr constant accumulation rate), represent the same type of depositional/erosional environment, a repeated climate signal. One can also assume, for example, that the 18 m separation corresponds to the perihelion cycle, giving a deposition rate of 0.36 mm/yr or to the long-term oscillations in eccentricity, giving a rate of 0.009 mm/yr. These layer sets become difficult to recognize in nearby image PSP_01738_2670 because of differing frost cover, so future analysis will include searching for more examples of packages of thin layers in other images.

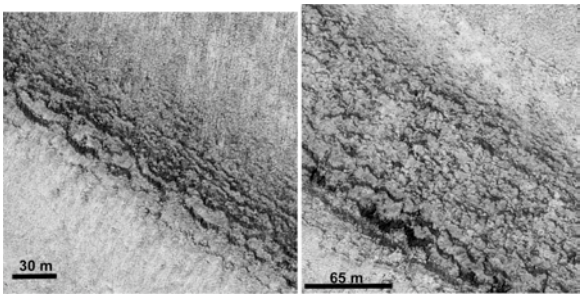

Fig. 5. Example of two sets of fine layering from one image (PSPS_01488_2665), possibly representing a repeating climate signal.

Layer Albedo: The intrinsic albedo of even the exposed surface of any of the layers is not easy to determine. It appears that layers are generally brightest on the tips of their hummocks and knobs and on the north- (up-trough-wall) facing side of ridges and slopes (Fig. 2). In general, layer brightness decreases down-section. These observations are consistent with several possibilities. 1) The layers are inherently dark, but frost collects on north facing slopes and increases in extent (and maybe thickness) further up-section, toward the top of the PLD. 2) The layers are inherently relatively bright, but as they sublimate in the summer, sublimation lag builds up in the hollows and in places protected from winds blowing off of the PLD surface and down the trough wall slope. In this case, the lag also tends to collect at the shallower slopes towards the bottom of the trough as it is removed from upper layers by wind and mass-wasting. 3) Or #2 is true in addition to the fact that surface frost increases up-section. If apparent layer albedo does not necessarily correspond, even qualitatively, to inherent layer composition, then models which tie PLD image

brightness profiles directly to changing orbital parameters [10, 11] may not be entirely realistic.

The Residual Ice Cap (NRC): As described in [4], the NRC is remarkably homogeneous at all observed scales, except for an apparent graben identified in MOC and MOLA data [17] and some rare impact craters. HiRISE clearly resolves the bumpy texture visible in MOC images into an undulating surface with mounds of frosted material interspaced with lows (Fig. 6), apparently created by coalesced pits. HiRISE color data show that the lows begin to defrost in late summer and that they have a color similar to the reddish portions of the underlying NPLD. This color similarity suggests that the NPLD is visible beneath the lows in the NRC and thus that the thickness of the NRC is small, contained almost entirely in the mounds. Given a mound height of about 1 m [18] and assuming 50% coverage by mounds, the NRC volume is < 420 km^3 (3.8 x 10^{14} kg for a pure water ice composition). This result has implications for Mars global climate models that include the NRC as a source of atmospheric water.

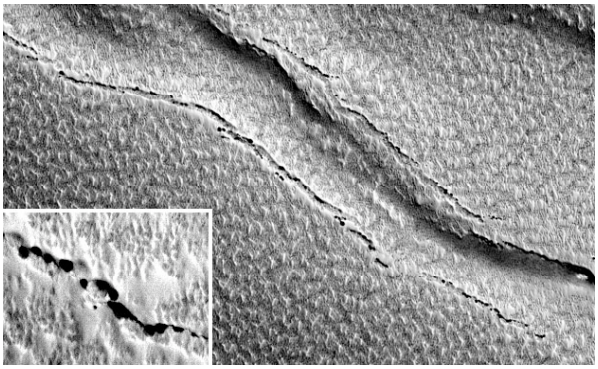

Fig. 6. Example of a portion of the NRC, showing typical undulating surface texture and a rare graben. Inset shows pits along graben walls. HiRISE image PSP_001513_2650, illumination from the top.

Geologic History: These HiRISE observations are consistent with the following general history of the north polar region [4]. Each of these steps can of course be divided into finer detail.

1) Dark sand saltating into the north polar region dominates deposition during periods (possibly of high obliquity and low regional ice stability) when thick accumulations of ice do not form [6, 5]. Alternating with these sand migration events, are times (possibly of low obliquity and high regional ice stability) when ice accumulates and inhibits saltation of underlying dark sand.

2) Several such depositional cycles produce alternating brighter (ice/dust) and darker (sandy) layers in the basal unit.

3) Transition to NPLD deposition occurs when the sand source is eventually exhausted and/or transport of sand into the north polar region ceases, or environmental conditions (possibly a lower average obliquity) change such that thick, dusty, ice accumulations are favored over cycles of sand and thinner ice deposition. The amount of intervening time between cessation of basal unit deposition and the beginning of NPLD deposition is unknown.

4) Varying conditions (possibly orbitally driven) during NPLD accumulation lead to the development of the traditional ice/dust layering, including deposition of layers identifiable NPLD-wide [11, 19] and the development of fractures and steeper slopes within the lower NPLD.

5) The NRC forms on top of the NPLD and evolves to its present state by condensation and sublimation of water ice.

6) Erosion of the NPLD and basal unit leads to accumulation of debris fans, avalanche deposits, and fallen blocks on the basal unit scarp [1], and to reworking of the sandy material into dunes to form the polar erg [6, 7, 5].

References: [1] Russell, P., et al. (2007), *7th International Mars Conference*, this volume. [2] Tanaka, K., et al. (2005), U. S. Geol. Surv. *Sci. Invest. Ser.* Map *288*. [3] Tanaka, K. and M. Bourke (2007), *Lunar Planet. Sci.*, *38*, Abs. 1856. [4] Herkenhoff, K., et al. (2007), *Science*, *submitted*. [5] Fishbaugh, K. and J. Head (2005), *Icarus*, *174 (2)*, 444-474. [6] Byrne, S. and B. Murray (2002), *J. Geophys. Res.*, *107 (E6)*, 10.1029/2001JE001615. [7] Edgett, K., et al. (2003), *Geomorph.*, *52*, 289-297. [8] Philipps, R. and e. al. (2007), *Lunar Planet. Sci.*, *38*, Abs. 1925. [9] Cutts, J. and B. Lewis (1982), *Icarus*, *50*, 216-244. [10] Laskar, J., et al. (2002), *Nature*, *419*, 375-377. [11] Milkovich, S. and J. Head (2005), *J. Geophys. Res.*, *110 (E05)*, doi: 10.1029/2004JE002349. [12] Malin, M. and K. Edgett (2001), *J. Geophys. Res.*, *106 (E10)*, 23,429-23,570. [13] Picardi, G. and colleagues (2005), *Science*, *310 (5756)*, 1925-1928. [14] Phillips, R. and e. al. (2007), *Lunar Planet. Sci.*, *38*, Abs. 1925. [15] Plaut, J. and colleagues (2007), *Science Express*, doi: 10.1126/science.1139672. [16] Milkovich, S. and J. Head (2006), *Mars*, *2*, 21-45. [17] Nunes, D., et al. (2006), *Eos Trans. AGU*, *87*, Abs. P31B. [18] Herkenhoff, K., et al. (2002), *Lunar Planet. Sci.*, *33*, Abs. 1714. [19] Fishbaugh, K. and C. Hvidberg (2006), *J. Geophys. Res.*, *111 E06012*, doi: 10.1029/2005JE002571.